

Experimental Challenges of the N* Program

R.W. Gothe

University of South Carolina, Department of Physics and Astronomy, Columbia, SC 29208, USA

Abstract. The first challenge faced in investigating the strong interaction from partially explored, where meson-cloud degrees of freedom dominate, to still unexplored distance scales, where the dressed-quark contributions are the dominating degrees of freedom, is to find an experiment that allows to measure observables that are probing this evolving nonperturbative QCD regime over the full range. Baryon spectroscopy can establish more sensitively, and in an almost model-independent way, nucleon excitation and non-resonant reaction amplitudes by complete measurements of pseudo-scalar meson photoproduction off nucleons. Elastic and transition form factors can then trace this evolution by measurements of elastic electron scattering and exclusive single-meson and double-pion electroproduction cross sections off the nucleon that will be extended to higher momentum transfers with the energy-upgraded CEBAF beam at JLab to study the dressed quark degrees of freedom, where their strong interaction is responsible for the ground and excited nucleon state formations. After establishing unprecedented high-precision data, the imminent next challenge is a high-quality analysis to extract these relevant electrocoupling parameters for various resonances that then can be compared to state of the art models and QCD-based calculations. Recent results demonstrate the status of the analysis and pinpoint further challenges, including those to establish QCD-based results directly from the experimental data.

Keywords: Baryon structure, constituent quark structure, strong degrees of freedom.

PACS: 13.40.Gp, 13.60.Le, 14.20.Gk.

INTRODUCTORY CHALLENGES

Already in the early inclusive high-energy deep inelastic scattering (DIS) experiments at SLAC [1], scaling and quasi-free scattering off the constituent quarks became visible at the then highest beam energies of up to $E = 20 \text{ GeV}$ but still moderate four-momentum transfers of $Q^2 < 2 (\text{GeV}/c)^2$. In Fig. 1 the quasi-free peak becomes visible at high beam energies and high center-of-mass energies W , where the electrons scatter off constituent quarks. From the marked maximum value of the quasi-free peak, the constituent quark mass $m_q \approx 0.36 \text{ GeV}$ and the expectation value of the quark core radius or the confinement radius $r_c \approx 0.79 \text{ fm}$ can be estimated in direct analogy to the bound-nucleon mass and the nuclear radius in electron scattering off nuclei, both based on the underlying Fermi statistics. Figure 1 also shows how the quasi-free scattering starts to dominate the elastic and resonance contributions with increasing E and Q^2 . Mapping out this transition over Q^2 and W in detail generates the experimental foundation to investigate quark-hadron duality [2], scaling, the bound-quark structure, confinement, dynamical mass generation, and the structure of baryons. The accepted research proposal PR-09-003 at JLab [3], Nucleon Resonance Studies with CLAS12, will lay this experimental foundation to address in a unique way these most challenging questions in QCD. Properly extracting and interpreting the results from the measured electron scattering data, particularly for transition form factors to specific excited nucleon states, might

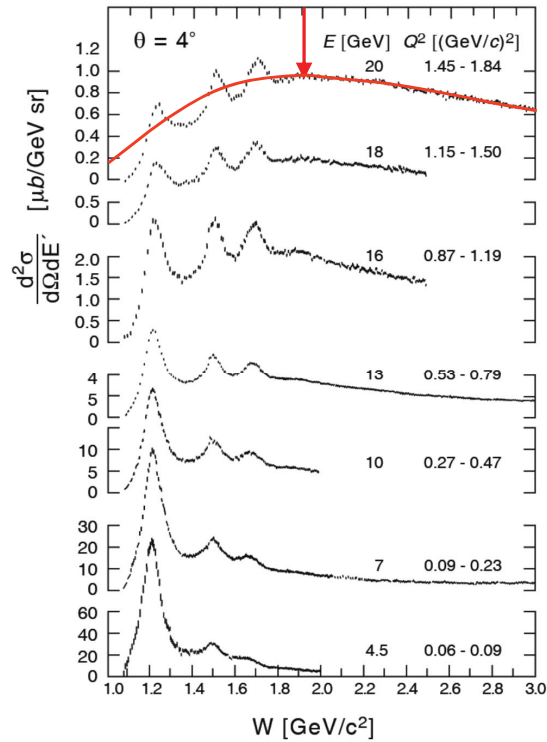


FIGURE 1. Experimental cross section values versus missing mass for early deep inelastic scattering experiments [1]. Sketched and marked at $E = 20 \text{ GeV}$ the partonic quasi-free electron scattering peak.

even pose a greater challenge than the measurement itself. More measured data on baryon spectroscopy and elastic form factors are needed to ease this process. A steadily growing collaboration of experimentalists and theorists is working together to enable the measurements, the analysis of the data, and the QCD-based interpretation of the results. The corresponding theoretical progress and challenges have last been documented in [4] and summarized in this conference [5]. This overview tries to highlight the experimental challenges of the N^* program and does not even attempt to be complete, but within the productive and well-organized NSTAR 2011 workshop the status of the N^* program was discussed in detail, which should also be reflected in these proceedings.

SPECTROSCOPIC CHALLENGES

The success of quantum electrodynamics was primarily based on the measurement of the spectrum of the excited hydrogen states, where hydrogen is the simplest atom bound by electromagnetic fields, whose ground state can be unambiguously described by its spectrum of excited states. In analogy one was hoping that by measuring the excitation spectrum of the simplest baryon bound by strong fields, one could understand the structure of the nucleon; and indeed, a large portion of the nuclear physics community enthusiastically started to investigate baryon resonances as new optimized detector sys-

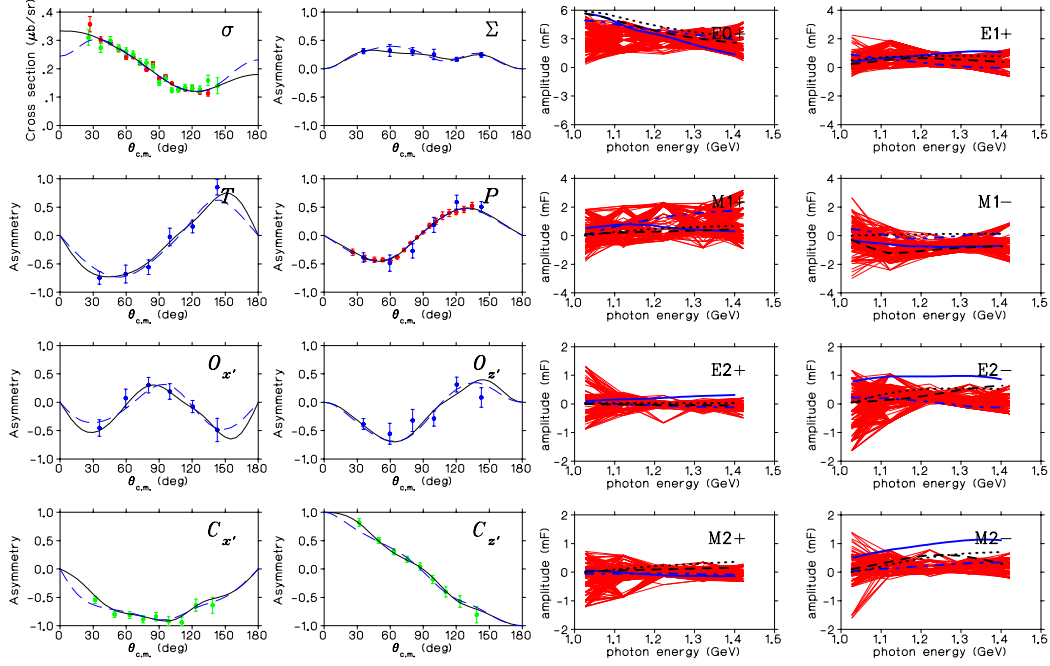


FIGURE 2. Left side: measured polarization observable data points σ , P CLAS-g11a [7] (red), Σ , T , P , $O_{x'}$, $O_{z'}$ GRAAL [8] (blue), and σ , $C_{x'}$, $C_{z'}$ CLAS-g1c [9] (green) are compared to the largest (dashed) and best $\chi^2/d.p.$ fit (solid line) for $W = 1883 \text{ MeV}$. Right side: solution bands (red) for the real parts of lowest lying PWA multipoles are compared to the BoGa [10] (dash-dotted), Kaon-MAID [11] (dashed), SAID [12] (dotted) and JLST [13] (solid lines). [6]

tems with large solid angle and momentum coverage and new high-intensity continuous electron beams became available at many facilities as ELSA, GRAAL, JLab, LEGS, MAMI, and others world wide. The high versatility of the provided electromagnetic probe, which has negligible initial state interaction, has produced intriguing results ever since. It was realized that the isoscalar or isovector and the electric, magnetic, or longitudinal nature of the coupling to hadronic matter probes different aspects of the strong interaction. However, the desired versatility of the electromagnetic probe comes with the complication that it mixes all these different coupling amplitudes, each with various resonance and background contributions, simultaneously into the measured cross sections. The best possible approach to disentangle all these interfering amplitudes is to carry out so-called complete experiments. In the simplest case of pseudo-scalar meson photoproduction, the cross section can be decomposed into four gauge- and Lorentz-invariant complex amplitudes. In a combination of unpolarized, beam-, target-, and recoil-polarization experiments, a total of up to 16 observables can be measured, of which only eight can be linearly independent. Particularly helpful here is that some weak hyperon decays have large analyzing power, which can replace the explicit recoil polarization measurement. Large solid angle detectors with high angular resolution are needed to separate the polarization observables by the azimuthal- and the partial waves by the polar-angle cross section distributions. Limited coverage, precision, and statistics will restrict the accuracy of the partial wave analysis (PWA) multipoles more and more

severely with growing relative angular momentum l , demanding, even in the simplest and best possible case of complete experiments, truncation of higher waves or other model-dependent assumptions.

In a recent topical review [6] the progress in the analysis of complete experiments is exemplified by the multipole extraction for the $\gamma p \rightarrow K^+ \Lambda$ reaction. Figure 2 shows a typical fit to the polar-angle distribution of the eight measured polarization observables and the corresponding solution bands for the real parts of the lowest partial wave multipoles. The width of the solution band depends not only on the uncertainty of the experimental data point, and hence again on the angular coverage, precision, and statistics of the experiment, but also on the number of measured polarization observables. The authors conclude that based on the eight measured polarization observables the predicted $D_{13}(1895)$ resonance contributions to the E_{2-} and M_{2-} PWA multipoles can be excluded, while P_{13} contributions to E_{1+} and M_{1+} can still not be validated in this W range. This situation will change when data for all 16 polarization observables within expected uncertainties become available, which would reduce the solution bandwidth for all shown multipoles (see Fig. 2) by roughly a factor of two, allowing to pinpoint the nature of new resonance contributions in the $K^+ \Lambda$ channel.

With the caveat that most baryon resonances, except the lowest lying ones, decay dominantly into vector-meson or multi-meson channels, complete experiments on single pseudo-scalar meson photoproduction and PWA will allow for the highest quality extraction of resonance parameters under minimal model assumptions.

HADRONIC STRUCTURE CHALLENGES

Beyond baryon spectroscopy at the real photon point $Q^2 = 0 (GeV/c)^2$, electron scattering experiments also investigate the internal hadronic structure at various distance scales by tuning the four-momentum transfer from $Q^2 \approx 0 (GeV/c)^2$, where the meson cloud contributes significantly to the baryon structure, over intermediate Q^2 , where the three constituent-quark core starts to dominate, to Q^2 up to $12 (GeV/c)^2$, attainable after the $12 GeV$ upgrade at JLab, where the constituent quark gets more and more undressed towards the bare current quark (see Fig. 4) [14, 27]. Although originally derived in the high Q^2 limit, constituent counting rules describe in more general terms how the transition form factors and the corresponding helicity amplitudes scale with Q^2 dependent on the number of effective constituents. Recent results for $Q^2 < 5 (GeV/c)^2$ [15, 20] indicate for some helicity amplitudes, like $A_{1/2}$ for the electroexcitation of the $N(1520)D_{13}$, the onset of proper scaling assuming three constituent quarks. This further indicates that in this case the meson-baryon contributions become negligible in comparison to those of a three constituent-quark core, which coincides nicely with the EBAC dynamical coupled channel calculation shown in Fig. 3 (right).

Along the same line of reasoning perturbative QCD (pQCD) predicts in the high Q^2 -limit by neglecting higher twist contributions that helicity is conserved. The fact that this predicted behavior sets in at much lower Q^2 values than expected [15] challenges our current understanding of baryons even further. For $N(1520)D_{13}$ the helicity conserving amplitude $A_{1/2}$ starts to dominate the helicity non-conserving amplitude $A_{3/2}$ at $Q^2 \approx 0.7 (GeV/c)^2$, as typically documented by the zero crossing of the corresponding helic-

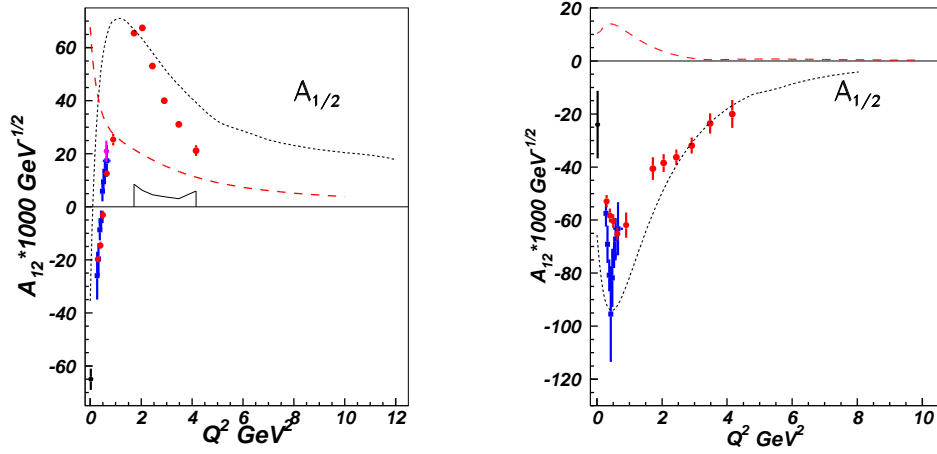


FIGURE 3. The contributions from quark degrees of freedom and meson-baryon dressing to the $A_{1/2}$ electrocouplings of the $P_{11}(1440)$ (left) and $D_{13}(1520)$ (right) states. The CLAS data from analyses of $N\pi$ [15] and $\pi^+\pi^-p$ [16] electroproduction are shown in red and blue, respectively. The contributions from the quark core, estimated within the framework of relativistic quark models [17, 18], are given by the dotted lines, and the absolute value of the contributions from meson-baryon dressing, obtained within the framework of the EBAC-DCC approach [19], are represented by the red (dashed) lines.

ity asymmetry $A_{hel} = (A_{1/2}^2 - A_{3/2}^2)/(A_{1/2}^2 + A_{3/2}^2)$. The $N(1685)F_{15}$ resonance shows a similar behavior with a zero crossing at $Q^2 \approx 1.1 (\text{GeV}/c)^2$, whereas the $\Delta(1232)P_{33}$ helicity asymmetry stays negative with no indication of an upcoming zero crossing; and even more surprising are the preliminary results for the $N(1720)P_{13} A_{1/2}$ amplitude, which decreases so rapidly with Q^2 that the helicity asymmetry shows an inverted behavior with a zero crossing from positive to negative around $Q^2 \approx 0.7 (\text{GeV}/c)^2$ [21]. This essentially different behavior of resonances underlines that it is necessary but not sufficient to extend the measurements of only the elastic form factors or the transition form factors to a well known resonance like the $\Delta(1232)P_{33}$ to higher momentum transfers. To comprehend QCD at intermediate distance scales where dressed quarks are the dominating degrees of freedom and to explore interactions of dressed quarks as they form various baryons in distinctively different quantum states, the Q^2 evolution of exclusive transition form factors to various resonances up to $12 (\text{GeV}/c)^2$ are absolutely crucial. Figure 3 exemplifies the three corner stones of the status quo in this baryonic structure analysis endeavor. First, the analysis of the $N\pi$ channel data is carried out in two phenomenologically different approaches based on fixed- t dispersion relations and a unitary isobar model [15, 22]. The main difference between the two approaches is the way the non-resonant contributions are derived. The $p\pi^+\pi^-$ CLAS data is analyzed within a phenomenological meson-baryon model [16, 23] that fits nine independent differential cross sections of invariant masses and angular distributions. The good agreement of the resonant helicity amplitude results in the single- and double-pion channels, that have fundamentally different non-resonant contributions, provides evidence for the reliable extraction of the $\gamma_v NN^*$ electrocoupling amplitudes. Second, the high Q^2 behavior is most consistently described by relativistic light-front quark models, like [17, 18, 24, 25],

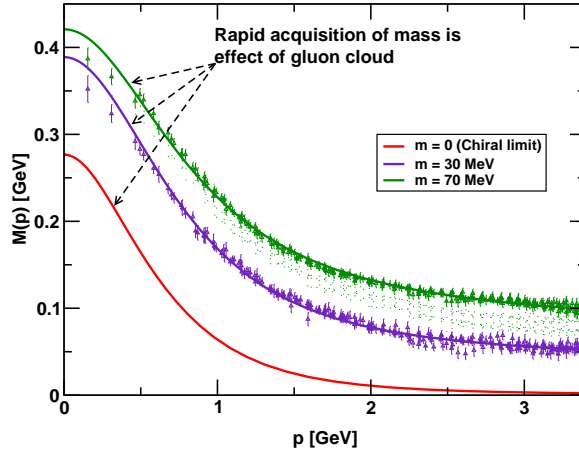


FIGURE 4. Dressed quark mass function, $M(p)$, for light-quarks, obtained in Landau gauge: solid curves are the DSE results, including the chiral-limit [27]; points with error bars are the results from unquenched LQCD [28]. The elastic and transition form factor data, that will become available after the 12 GeV upgrade, probes $M(p)$ up to a quark propagator momentum of $1.15\text{ GeV}/c$, which spans the transition from dressed constituent quarks to the almost-completely undressed current quarks.

but their description of the low Q^2 behavior is less satisfactory. Third, the Excited Baryon Analysis Center (EBAC) predicts, based on a full dynamical coupled-channel analysis [26], meson-baryon dressing (meson-cloud) contributions that seem to bridge the gap [4] between the relativistic light-front quark models and the measured results at low Q^2 . Digging deeper into the baryonic structure by increasing the momentum transfer beyond $5(\text{GeV}/c)^2$ [3] opens a unique window to investigate the dynamic momentum-dependent structure of the constituent quarks. This becomes apparent in Fig. 4, where the quark mass function for momenta larger than $2\text{ GeV}/c$ describes a current-quark that propagates almost like a free single parton. However, for momenta less than that, the quark mass function rises sharply, entering the confinement regime and reaching the constituent-quark mass scale in the infrared. In this domain, the quark is far from being a single parton and is dressed by a cloud of low-momentum gluons attaching themselves to the current-quark, which is a direct manifestation of dynamical chiral-symmetry breaking.

SUMMARY

All visible matter that surrounds us is made of atoms, which are made of electrons and nuclei; the latter are made of nucleons, which are finally made of quarks and gluons. Contrary to the most recent discussions in the news, the Higgs, or more frequently called the God Particle, is not responsible for the generation of all mass. It is already known that 98% of all visible mass is generated by strong fields. Establishing an experimental and theoretical program that provides access to

- the dynamics of nonperturbative strong interactions among dressed quark, their emergence from QCD, and their confinement in baryons,

- the dependence of the light quark mass on the momentum transfer and thereby how the constituent quark mass arises from dynamical chiral-symmetry breaking, and
- the behavior of the universal QCD β -function in the infrared regime,

is indeed most challenging on all levels, but recent progress and future commitments bring a solution of these most fundamental remaining QCD problems into reach.

Single-, double-, and triple-polarization experiments are essential to establish anchor points for the most detailed separation of individual resonance and background contributions. Elastic and particularly transition form factors are then uniquely accessing nonperturbative QCD from long to short distance scales.

ACKNOWLEDGMENTS

This work was supported in part by the National Science Foundation, the U.S. Department of Energy, and other international funding agencies supporting research groups at Jefferson Lab.

REFERENCES

1. S. Stein et al., Phys. Rev. **D 12** (7), 1884-1919 (1975).
2. E.D. Bloom and F.J. Gilman, Phys. Rev. Lett. **25** (16), 1140-1144 (1970) and Phys. Rev. **D 4** (9), 2901-2916 (1971).
3. R.W. Gothe, V. Mokeev, et al., “Nucleon Resonance Studies with CLAS12”, Approved Proposal E-09-003 and Update, www.physics.sc.edu/~gothe/research/pub/nstar12-12-08.pdf (2009) and www.physics.sc.edu/~gothe/research/pub/ns12-2010-01-05.pdf (2010).
4. I.G. Aznauryan et al., “Theory Support for the Excited Baryon Program at the Jlab 12 GeV Upgrade”, arXiv:0907.1901v3 [nucl-th], 1-53 (2009).
5. C.D. Roberts, these proceedings (2011).
6. A.M. Sandorfi et al., J. Phys. G: Nucl. Part. Phys. **38** 053001 (2011).
7. M.E. McCracken et al., Phys. Rev. **C 81** 025201 (2010).
8. A. Lleres et al., Eur. Phys. J. **A 31** 79 (2007) and Eur. Phys. J. **A 39** 149 (2009).
9. R.K. Bradford et al., Phys. Rev. **C 75** 035205 (2007) and Phys. Rev. **C 73** 035202 (2006).
10. A.V. Anisovich et al., Eur. Phys. J. **A 44** 203 (2010).
11. MAID and Kaon-MAID isobar models, www.kph.uni-mainz.de/MAID/ (2011).
12. SAID partial wave analysis, <http://gwdac.phys.gwu.edu/> (2011).
13. B. Julia-Diaz et al., Phys. Rev. **C 73** 055204 (2006).
14. I.G. Aznauryan et al., J. Phys. Conf. Ser. **299** 012009 (2011).
15. I.G. Aznauryan et al., Phys. Rev. **C 80** 055203 (2009).
16. V.I. Mokeev et al., arXiv:0906.4081[nucl-ex] (2009) and these proceedings (2011).
17. I.G. Aznauryan, Phys. Rev. **C 76** 025212 (2007).
18. E. De Sanctis et al., Phys. Rev. **C76** 062201 (2007).
19. B. Julia-Diaz, T.-S.H. Lee et al., Phys. Rev. **C77** 045205 (2008).
20. K. Park et al., Phys. Rev. **C 77** 015208 (2008).
21. V.I. Mokeev, arXiv:1010.0712[nucl-ex] (2010).
22. I.G. Aznauryan, Phys. Rev. **C 67** 015209 (2003).
23. V.I. Mokeev et al., Phys. Rev. **C 80** 045212 (2009).
24. S. Capstick and B.D. Keister, Phys. Rev. **D 51** 3598 (1995).
25. H.J. Weber, Phys. Rev. **C 41** 2783 (1990).
26. A. Mastsuyama et al., Physics Reports **439** (2007).
27. M.S. Bhagwat et al., Phys. Rev. **C 68** 015203 (2003) and AIP Conf. Proc. **842** 225 (2006).
28. P.O. Bowman et al., Phys. Rev. **D 71** 015203 (2005).